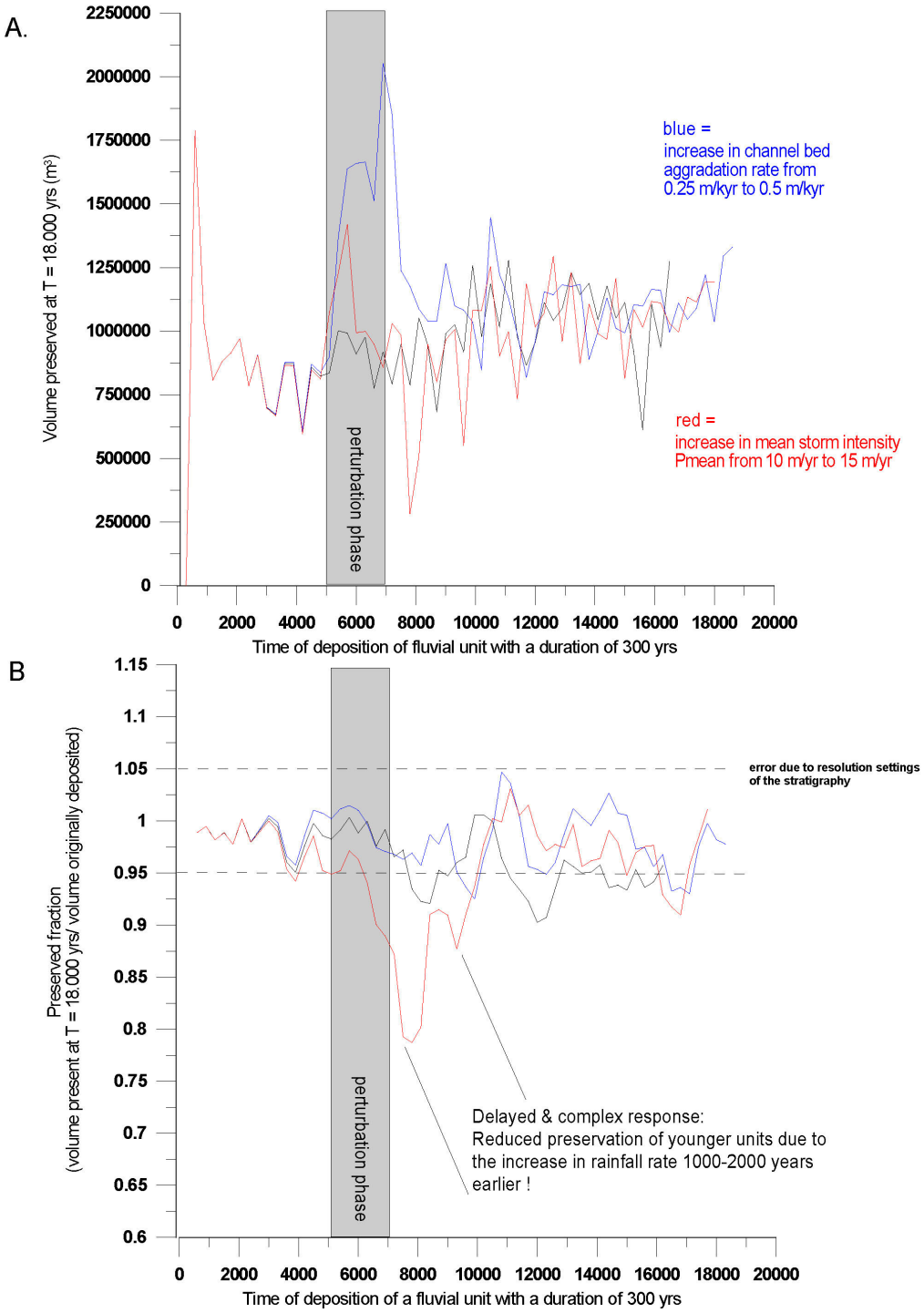

Figure 13. Preservation potential of fluvial units present in the subsurface at T = 18.000 yrs, as function of their age. Grey column represents a 2000 yr perturbation period, where the channel bed aggradation rate is increased (blue), and the storm intensity (red). A) preserved volume, B) Ratio of volume at T = 18.000 yrs/ undisturbed volume which was originally deposited. An increase in storm intensity (red) first results in a larger volume of preserved sediments, because the channel belt expands (Fig.11B) and a larger area is affected by floodplain sedimentation. However, units deposited some 1000 yrs after the perturbation are also affected by the storm intensification pulse. They have a poor preservation potential due to the increased meander migration rates (Fig. 12B), which are part of the transient response to the storm pulse.

6. Model runs set 2, Geoarchaeology

6.1 Geo-archaeological scenarios

The model operates at Holocene timescales and was used to study the distribution of archaeological units at the surface and subsurface. An example is given in figure 14, where the accumulated stratigraphy in the subsurface is sliced horizontally and presented as maps showing the ages of the sediment at 0.5, 1.0, 2.0 and 3.0 meters below the floodplain. The ages of these sediments are grouped and coloured according to the standard archaeological timescale for the British Isles.

For this experiment the model-starting surface consisted of a selection of the elevation model of a part Upper Thames Valley. An average Holocene sedimentation rate of this area of 0.25m /kyr was used to drive the channel bed aggradation rate.

At a depth of 0.5 m, just below the plough depth, the floodplain is predominantly of Roman age and contains some patches of younger Saxon and Medieval deposits at the right-hand side. These linear patches follow the strike of the undulating topography in the floodplain. The 0.5 m depth slice reveals the position of a Medieval paleo-channel At 1.0 m depth the floodplain is dominantly Bronze Age and the linear patches striking perpendicular to the channel are Iron Age.

All variables in the example of figure 14 were kept constant throughout the simulation and therefore the results of this experiment can be used for comparison to four additional scenarios characterised by more complex climatic histories (figure 15).

In the first of these scenarios the storm rainfall intensity was increased from 10 to 12.5 m/yr during distinct pulses, of which the duration and relative timing correspond to the Central European cold-humid phases of Haas et al. (1998), figure 15. All other important variables, such as overbank deposition rate μ, and channel aggradation rate were held constant at 0.20 and 0.25 m/kyr, respectively.

In the second scenario the overbank sedimentation rate μ was raised from 0.20 to 0.30 according to the timing of these phases, reflecting higher rates of sediment transport towards the floodplains during these wet periods. In the third scenario both the storm intensity and the overbank sedimentation rate were increased simultaneously. In addition, during this simulation the channel bed level of the river was raised artificially according to a stepwise increasing curve. The trend (Figure 15) is described by a slow channel bed aggradation rate during the Early Holocene (0.16 m/kyr) and a moderate raise since Bronze Age (0.25 m/kyr), reflecting the onset of

land use in upstream catchments. An even higher rate of channel bed aggradation rate

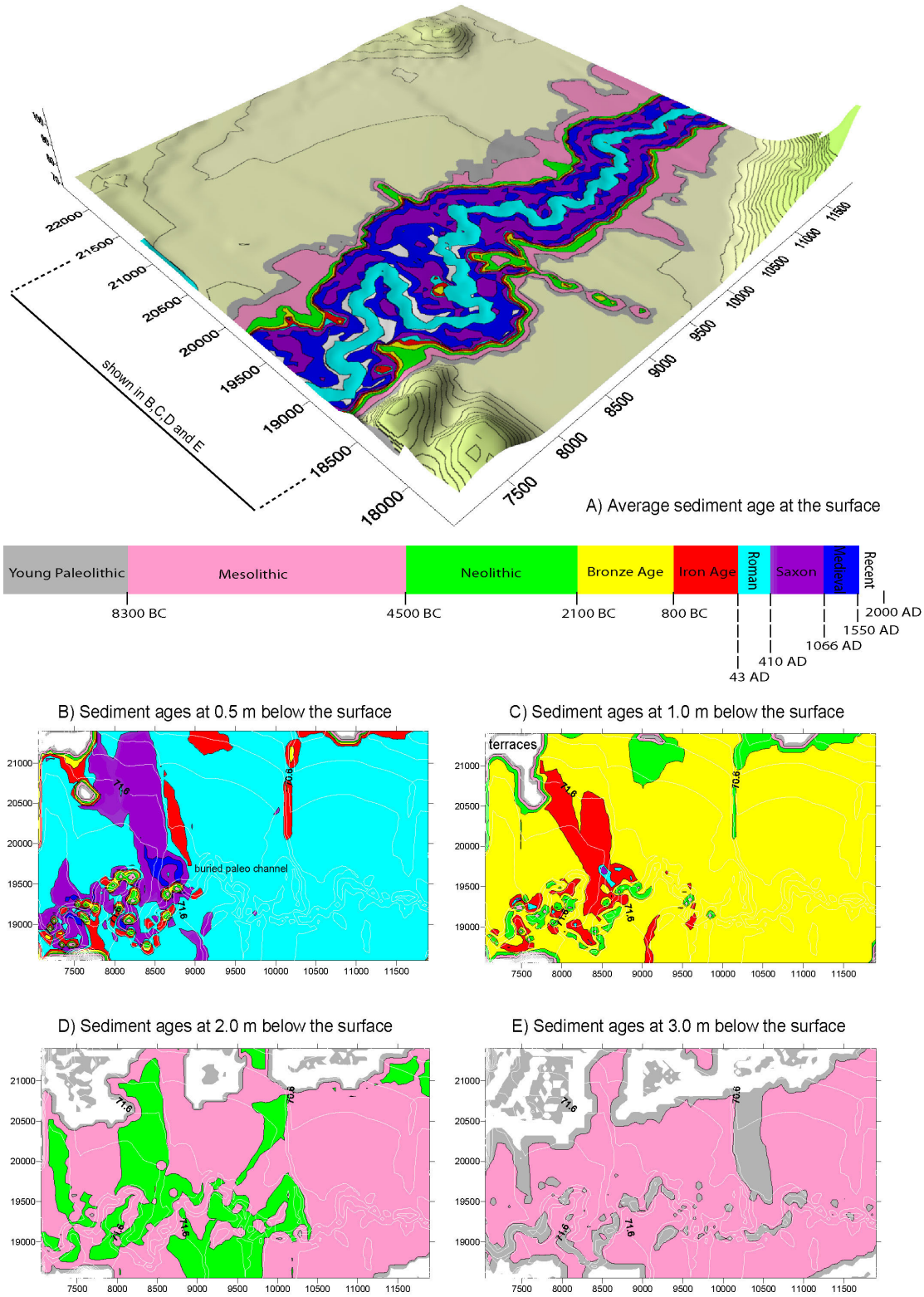

Figure 14. Subsurface maps showing the spatial distribution of archaeological important time slices at depths at 0.5, 1, 2 and 3 m below the floodplain surface.

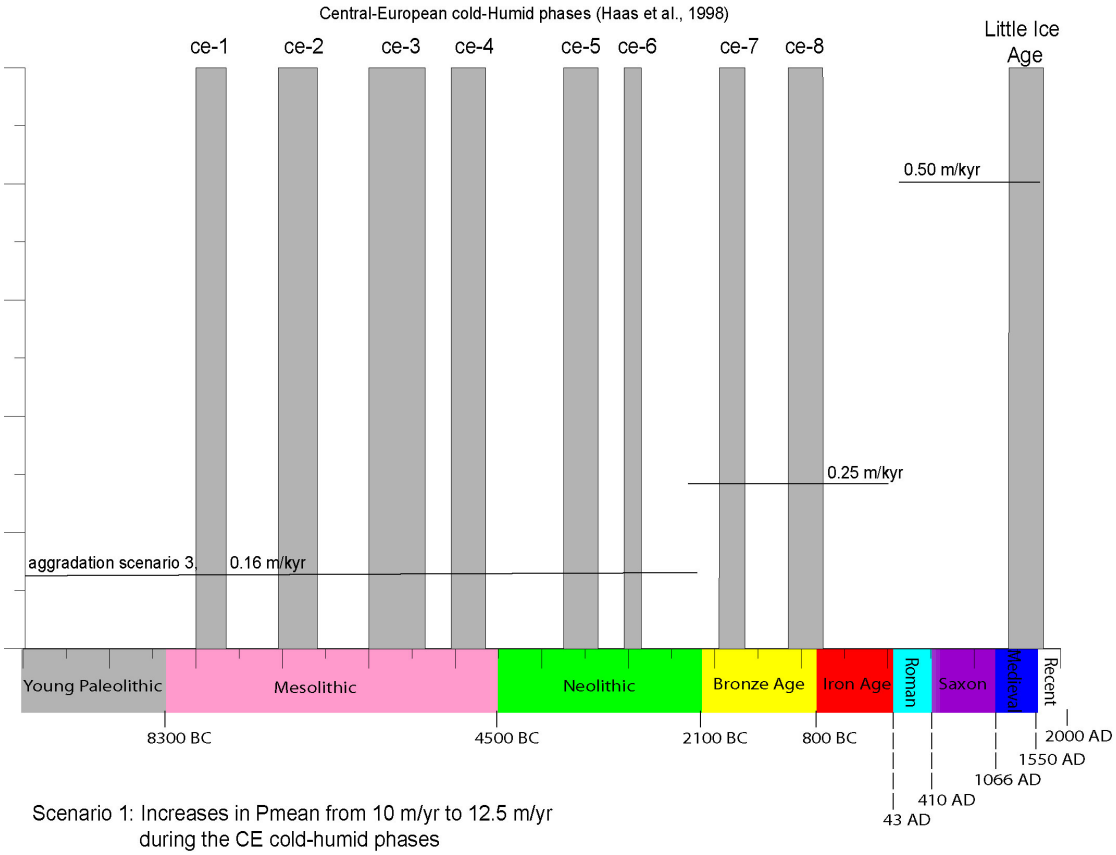

Scenario 1: Increases in Pmean from 10 m/yr to 12.5 m/yr during the CE cold-humid phases

Scenario 2: Increase in overbank sedimentation rate constant from 0.2 to 0.3 during the CE cold-humid phases

Scenario 3: Increase of Pmean and overbank sedimentation rate during the CE cold-humid phases, and a stepped increase of channel bed aggradation rate from 0.16 to 0.50 m/kyr.

Scenario 4: Alternating incision (- 0.1 m/kyr) and aggradation (0.8 m/kyr), where the aggradation periods correspond to the CE cold-humid phases.

Figure 15. Overview of the timing of the Central European Cold Humid phases of Haas et al., (1998) with respect to the archaeological timeslices used in the model scenarios.

(0.50 m/kyr) is applied from Roman times onwards, as this period is associated with the start of more efficient land use techniques, widespread erosion and high sediment flux to rivers (Lewin and Macklin, 2003). In the fourth and last scenario modelled the timing and duration of the European cold-wet phases was used to drive channel bed aggradation and incision rates. In this scenario high channel bed aggradation rates of 0.8 m/kyr correspond to the wet phases, whereas moderate incision is applied during dryer periods (-0.2 m/kyr), except for the Roman and post-Roman.

The resulting distribution of average ages in the top layers of the floodplain is very different for the four scenarios (figure 16). The range of surface ages generated by scenario 1 is diverse, whereas the other scenarios show a dominance of one time slice on the floodplain. In scenario 2, the floodplain is relatively young and dominated by Medieval deposits, due to the last increase in floodplain sedimentation rate during the Little Ice Age (Figure 15). The dominance of Bronze Age in the surface of scenario 3 is the effect of the increased channel bed aggradation rate from 0.16 to 0.25 m/kyr during this period. In the surface of scenario 4 the floodplain width is much narrower, and the surface shows more timeslices close to the channel. Again the Bronze Age sediments are pronounced, and also in this scenario this is caused by the high channel bed aggradation rate events during this period.

The age maps were also made for the subsurface slices, figure 17. Depth-age maps for scenario 1 and scenario 2 are dominated by a combination of Roman and Saxon at 0.5 m the below the floodplain and traces of Neolithic to Iron Age are exposed at the cut banks of the channel. The subsurface results of these two scenario are very similar, but in the subsurface of scenario 3 the first meter below the subsurface is much younger, due to the post-Roman increases of channel bed aggradation rate (Figure 15). The opposite holds for the subsurface of scenario 4, where occasional phases of incision generated less complete sediment volume for the more recent period, and Bronze and Iron Age deposits can be found directly under the floodplain surface. Here the Roman and Medieval sediments are only present close to the channel.

Another special nature of scenario 4 is recognisable in the preservation potential curves (figure 17). Most of the alluvial units accumulated during the course of the four scenarios have a high degree of preservation. Almost none of the alluvial units of scenarios 1, 2 and 3 are eroded or reworked for more than 20%, whereas in scenario 4 especially the older units have a low preservation potential.

An additional characteristic that can be read from theses curves that there is no clear correlation between the timing of the cold-humid phases applied, the development of the river sinuosity and the preservation potential of the sediments. Most likely channel response interference patterns prevent this.

It can be concluded from the scenarios that for constantly aggrading floodplains, Holocene centennial scale variations in rainfall or overbank deposition supply are difficult to recognize in stratigraphic data (Figure 17) or preservation potential

statistics (Figure 18). Patterns generated by variations in channel aggradation rate and especially incision leave a much clearer mark on the stratigraphy.

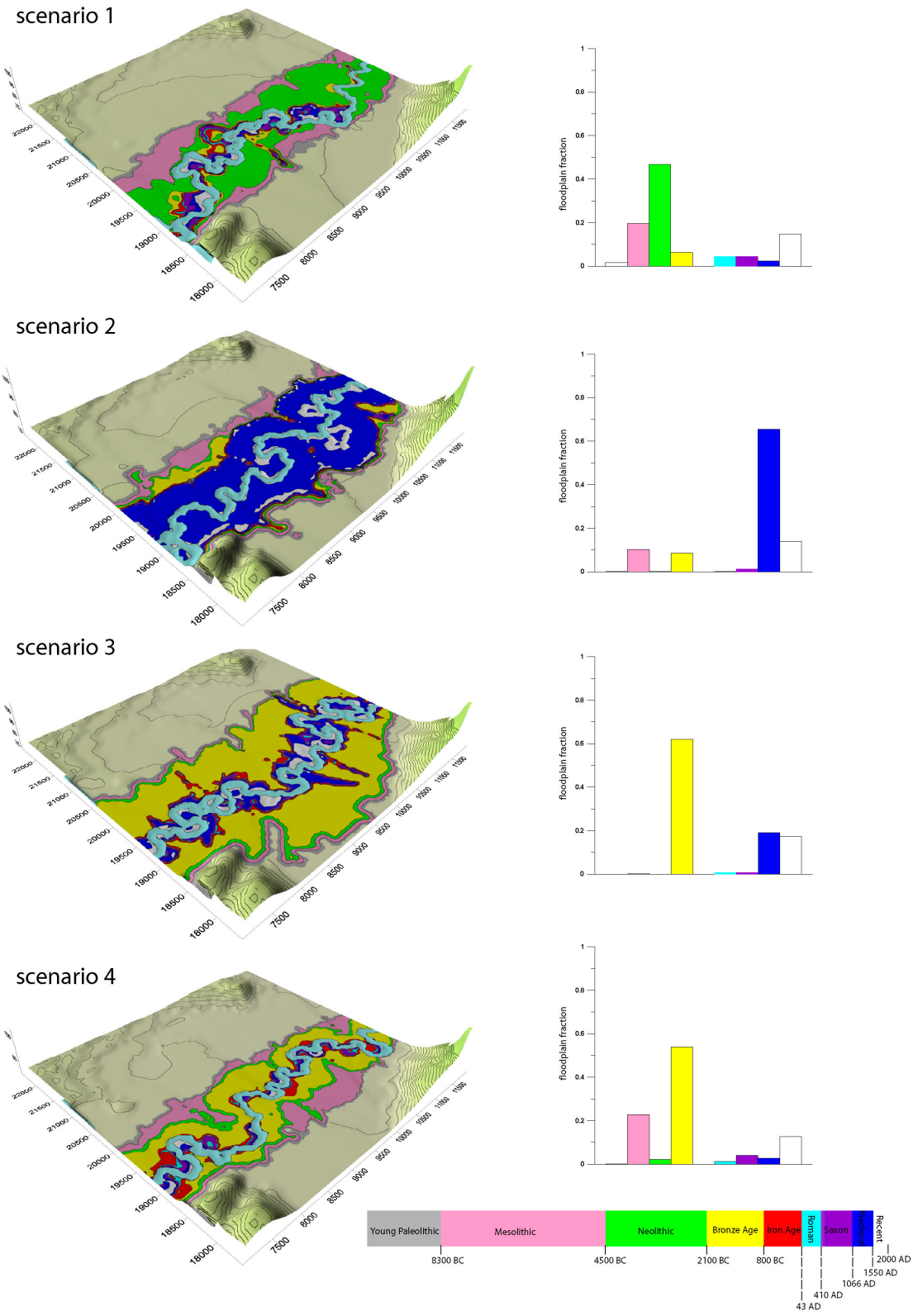

Figure 16. Ages of the sediment in the top layer of the floodplain for four of the climate-landuse scenarios modelled.

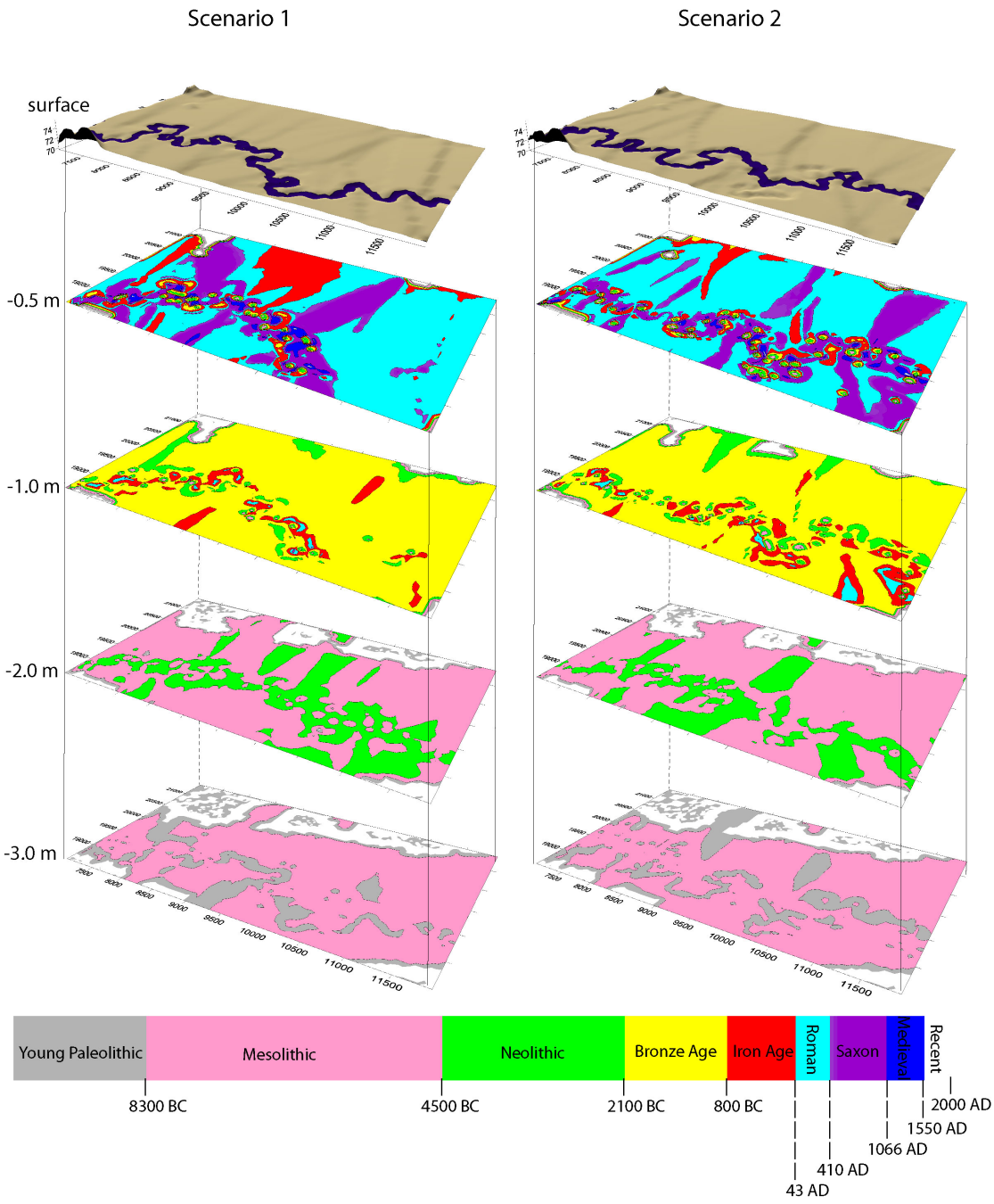

Figure 17. Sediment ages at depths of 0.5, 1, 2 and 3 meter below the floodplain surface for scenario 1 and 2.

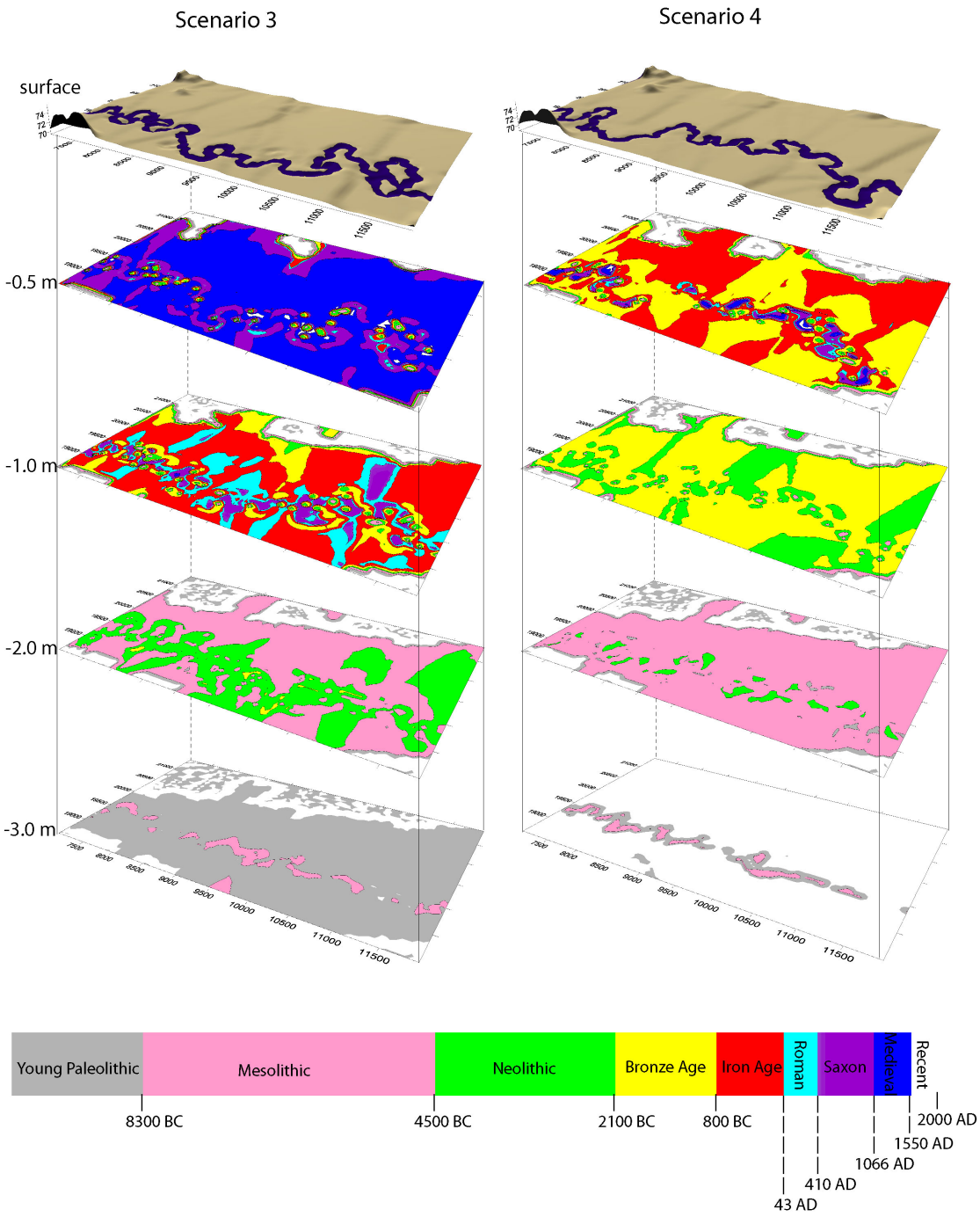

Figure 17. Sediment ages at depths of 0.5, 1, 2 and 3 meter below the floodplain surface for scenario 3 and 4.

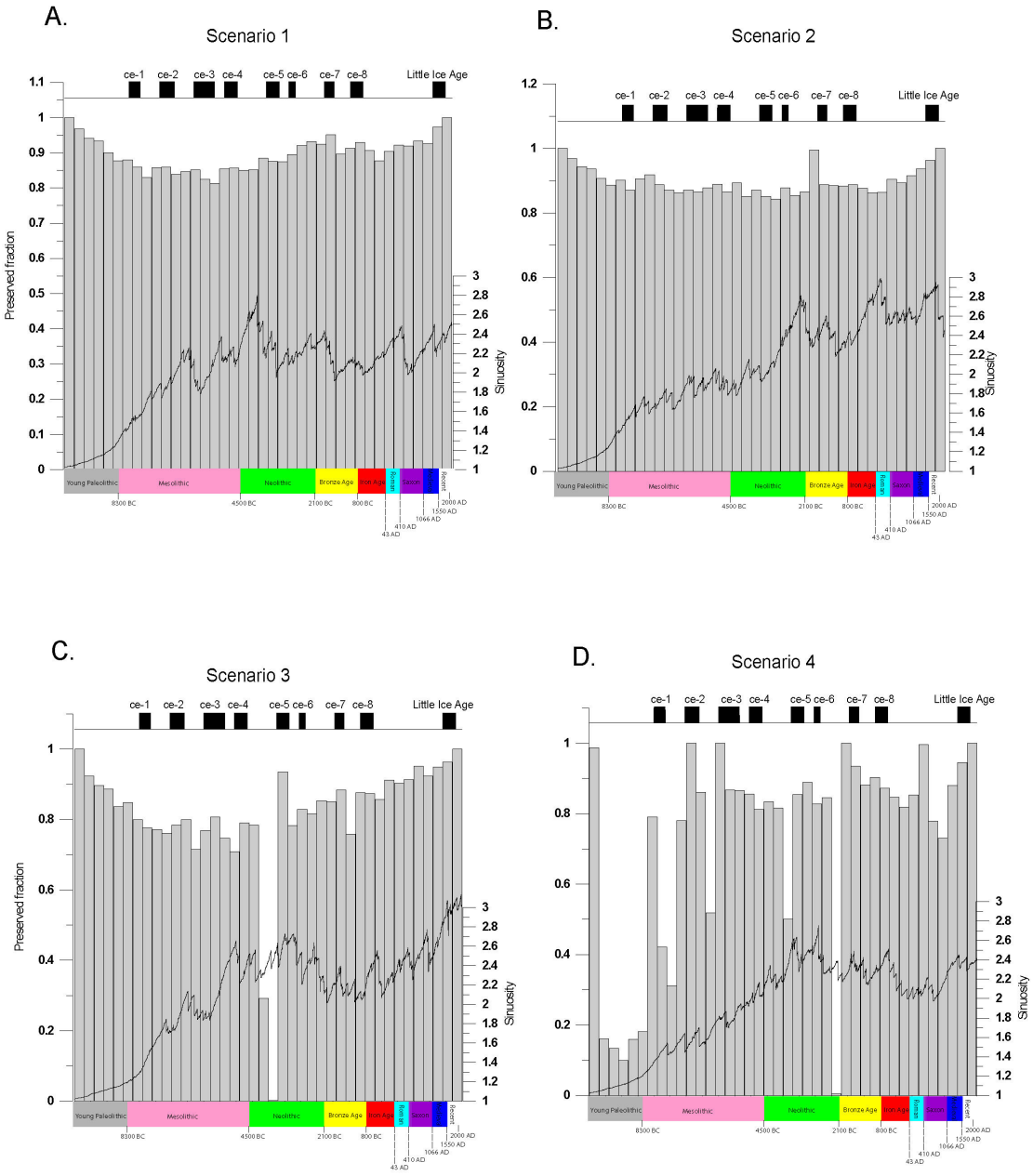

Figure 18. Preservation potential curves for the stratigraphic units accummulated during scenarios 1-4.

Ultimately, the subsurface distributions of sediment ages generated by the model could be compared to a study of a real floodplain using sediment cores and dating techniques, in order to verify the algorithms and the input variables used in the scenarios. In cases where the model results seem to match observed subsurface data, these same model results might be used to aid further archaeological prospecting. This can be done in a straightforward sense by 'following' the matching depth-age maps, but also indirectly using transition matrices. These matrices summarize the probability

of finding a certain a timeslice in a given direction based on the known age of the sediment at a specific location.

7. Dissemination of results

The improved meander-floodplain model and the results of the experiments were presented at the American Geophysical Union Fall Conference, 2003 in San Francisco and at a conference on 3D stratigraphic modelling and prediction for the aggregates and oil industry in Utrecht, the Netherlands. The report and posters are available this week for downloading from the research website, together with a selection of key figures and animations for outreach purposes. Furthermore, a paper discussing the numerical method and experimental results has been completed and submitted to the Utrecht conference special volume.

8. References

Fenner E. P. and Dyer C.A. (1994) The Thames Valley Project; A report for the National Mapping Programme. Air Photography Unit, Royal Commission on the Historical Monuments of England. pp. 185

Haas JN, Richoz I, Tinner W, Wick L. (1998). Synchronous Holocene climatic oscillations recorded on the Swiss Plateau and at timberline in the Alps. The Holocene 8 (3): 301–309.

Howard, A.D. (1992) Modelling channel migration and Floodplain sedimentation In: Lowland Floodplain Rivers; Geomorphological perspectives (Carling, P.A. and Petts, G.E., eds) pp. 1-41

Howard, A. D., (1996). Modelling channel evolution and floodplain morphology, in *Floodplain Processes*, edited by M. G. Anderson, D. E. Walling, and P. D. Bates, pp. 15–62, Wiley, Chichester,

Ikeda, S. (1989) Sediment transport and sorting at bends. In River meandering, Ikeda S., Parker, G. (eds) American Geophysical Union: Washington, p.181-214

Johannesson, H. and G. Parker (1989) Linear theory of river meanders, chapter 7 in *RiverMeandering*, edited by S. Ikeda and G. Parker, *Water resources monograph*, *12*, pp. 181–212, American Geophysical Union.

Lancaster S.T. and Bras R.L., (2002) A simple model of river meandering and its comparison to natural channels, Hydrological Processes, 16, 1-26.

Lancaster, S.T. (1989) A nonlinear river meandering model and its incorporation in a landscape evolution model, PhD thesis, Department of Civil and Environmental Engineering, Massachusetts Institute of Technology, Cambridge, Boston pp. 277

Lewin, J. and Macklin, M.G. (2003) Preservation potential for late Quarternary river alluvium. Journal of Quarternary Science,18(2), pp. 107-120

Smith, J.D. and McLean, S.R (1984) A model for flow in meandering streams Water Resources Research 20(9); 130-1315

Sun T., Meakin, P., Jossang, T., Schwarz, K. (1996) A simulation model for meandering rivers. Water Resources Reseacrh 32(9): 2937-2954

Tucker, G.E., Lancaster, S.T., Gasparini, N.M., and Bras, R.L. (2001) The Channel-Hillslope Integrated Landscape Development (CHILD) Model, in *Landscape Erosion and Evolution Modeling,* edited by R.S. Harmon and W.W. Doe III, Kluwer Academic/Plenum Publishers, pp. 349-388

Mackey S.D., and Bridge J.S. (1995) Three-dimensional model of alluvial stratigraphy: theory and application. Journal of Sedimentary Research, B65:7-31

Needham, S. (1992) Holocene alluviation, interstratified settlement evidence in the Thames Valley at Runnymede Bridge. In alluvial Archaeology in Britain, Needham, S. and Macklin MG (eds). Oxbow Monograph 27: Oxford; 197-208

Contact Details

Quintijn Clevis

School of Geography and the Environment
Mansfield Road, OX1 3TB, Oxford, UK
Tel. 01865-71913
e-mail: quintus.clevis@geog.ox.ac.uk

From 4/15/2004
Dept. of Geological Sciences
Cooperative Institute for Research in Environmental Sciences
University of Colorado
Boulder, CO 80309-0399, USA